Original Paper

Characteristics of Deep-seated Landslide and Debris-flow Prevention Function of Cedar Forest

Learnings from Hirose Landslide, Ishikawa Prefecture, Japan

Prakash S. Thapa[1], Kazeto Hanzawa[2], Naoya Katsumi[3], Toshihiko Momose[3], Seiji Yanai[4]

Abstract

In May 2021, a large-scale deep-seated landslide occurred in Hirose-town, Hakusan City, Ishikawa Prefecture in Japan. The landslide extended to an area of 1.1 hectares with a 22m deep scouring head scarp, producing approximately 86000m^3 sediment. The collapsed debris flowed about 475m distance downstream, destroying the planted Cedar (*Cryptomeria japonica*) forest on the slope, then outspread and ultimately deposited on the alluvial terraces downstream. The landslide removed an estimated 540 Cedar trees, each with an average height of 23.3 meters. At the deposition area, it was observed that the drifted trees accumulated to create a retention dam-like structure of 8m in height which obstructed huge sediment material behind it. The leading edge of the debris flow was almost captured within the tree line, and the gap of this outflow with the rice paddy field below was approximately 25m. This study concluded that the massive debris flow that would have otherwise reached the paddy fields was prevented by two factors: (a) the mature Cedar forest, which developed a resistive force that halted the energy of the debris flow, and (b) a natural retention dam-like structure formed by driftwood obstructed along the standing trees, which trapped numerous debris. Therefore, the findings of this research will enhance our understanding of the preventive functions of trees against debris flow in hillslopes.

Keywords：Deep-seated landslide, Cedar forest, driftwood dam, Debris-flow prevention functions, LiDAR

1. Introduction

Recently as a consequence of climate change, mountain landslides are occurring more frequently every year throughout Japan. In the year 2017, a large-scale mountain collapse hit a Cedar (*Cryptomeria japonica*) plantation forest area in the Kitakyushu area, and the debris flow caused damage to downstream communities (Asada et al., 2020). Also in 2018, the Chugoku region experienced torrential rains causing mountain slope failures and mudslides resulting in large landslides (Kaibori et al., 2018). The sediment disasters have been increasing in recent years. Though erosion control and flood control structures have been constructed to minimize these disasters, the percentage of countermeasures constructed in collapse-prone areas is extremely low.

A landslide is a complex phenomenon in which weathered soil layers or base rock on a slope lose stability due to heavy rainfall, and snow melting, etc. It can be divided into two types of collapse: shallow landslide (landslide of topsoil with 2-3 m depth from the ground surface) and deep landslide (relatively large-scale failure in which not only the topsoil layer but also a deep layer of ground up to several tens of meters in depth becomes a collapsed earth mass). In the past, surface failures used to occur more frequently in Japanese mountains (Yanai and Igarashi, 1990), but deep failures have become more frequent in recent years (Jitozono and Shimokawa, 1998; Matsumura et al., 2012), and there is much urgency in elucidating their mechanisms and predicting their occurrences.

When the landslide occurs at a much deeper surface than the root systems of trees, the soil-binding

[1] Doctoral Course, Division of Sciences for Bioproduction and the Environment, Graduate School of Bioresources and Environmental Sciences, Ishikawa Prefectural University
[2] Former undergraduate student (Batch of 2021), Department of Environmental Science, Faculty of Bioresources and Environmental Sciences, Ishikawa Prefectural University
[3] Department of Environmental Science, Faculty of Bioresources and Environmental Sciences, Ishikawa Prefectural University
[4] Professor Emeritus, Ishikawa Prefectural University
*Corresponding Author: Seiji Yanai (yanai@ishikawa-pu.ac.jp)

effect of tree root systems in preventing such landslide (Kitahara, 2010) is not observed. However, it has been reported that when collapsed soil flows downstream as debris flow, its energy is reduced by trees growing along the transportation and deposition areas as a natural barrier, resulting in a shorter-flow-distance (Mizuyama et al., 1990; Nonoyama et al., 2020). The purposes of this study are : (a) to illustrate the mechanism of deep-seated Hirose town landslide (hereafter known as Hirose Landslide), which occurred near human settlements and paddy fields in the spring season using aerial photos and Laser Imaging and Ranging (LiDAR) data, and, (b) to quantify the functions of Cedar trees to control debris flows.

The learnings of this study can be referred to create effective ecosystem-based disaster risk reduction (Eco-DRR) approaches in landslide-prone areas.

2. Research methods

(1) Study site

The Hirose Landslide that occurred on 20th May 2021, is situated in Hakusan city in Ishikawa prefecture, central Japan with a geographical location of 136^0 37′ 30.55″ E and 36^0 24′ 54.68″ N (Figure 1). It has an elevation range of 125m-385m with the land surface generally inclining from east to west. The area is located near a Hirose town settled on a river terraces on the left bank of Tedori river, which is 72km long perennial river that originates from Mt. Hakusan (2702m) and confluences in the Sea of Japan. The nearest settlement has 34 households living around and cultivating the alluvial fan for vegetables and paddies production.

In this area, distinct river terraces are formed along the Tedori River. River terraces have a specific height lesser than 10 m having a clear flat surface along the middle to lower reaches of the Tedori River (Ishikawa Prefecture, 1987). In the Hirose Landslide area, the terraces form a flat surface with a horizontal distance of about 500 m from the Tedori River, and mostly used as paddies production land. On the left bank of the Tedori River, where the landslide occurred in 2021, a hill range with an elevation of 300-400m has developed continuously for 4-5km parallel to the river, and the mountain slope is steep with an average gradient of 30°. Furthermore, a distinct alluvial cone topography, with a width of 100 meters and a 15-degree slope, is continuously formed along the boundary between the river terrace and the hill slope. The tip of this cone overhangs the river terraces, forming a fan shape (Figures 1 and 2). The upper part of the slope has a steep valley-like topography.

According to the surface geological map of the National Land Survey Office (Ishikawa Prefecture, 1987), the geology of the area is mostly composed of rhyolitic pumice tuff and hornblende tuff, which is generally light greenish gray in color. The rhyolite is exposed in various places and is often white in color due to alteration. The altered rhyolite is used as a ceramic ore. The ceramic stone which is the raw material for Kutani ware is mined at the Kawai Mine (Ishikawa Prefecture, 1987) located 3.5 km south of the Hirose Landslide area.

The existing vegetation on the hill-slope is Cedar plantations on the lower part of the slopes and dense secondary broadleaf forests on the upper part of the slopes. The planted Cedar Forest is about 60 years old, with an average diameter at a breast height (DBH) of 60 cm and a average height of 30 m, with some trees reaching 35 m. The trees are relatively well-grown and established in the Hirose Landslide surrounding. Secondary broadleaf forest at the upper slope to the ridge is composed mainly of *Quercus serrata*, and a variety of other broadleaf trees such as Japanese alder (*Alnus hirsuta*), Cherry (*Prunus serrulate*), azuki-nashi (*Aria alnifolia*), and Aburachan (*Parabenzoin praecox*), with medium diameter trees measuring 30 cm at breast height and 10 m or less in height. The forest-floor receives little light, and ferns grow in abundance throughout the landscape in the forest around the Hirose Landslide.

(2) Methods

1) Topographic assessment using LiDAR data

The topography before the collapse was reconstructed using airborne LiDAR data and aerial photographs taken in 2006, which were provided by the Kanazawa office of Rivers and National Highways, Ministry of Land Infrastructure, Transport, and Tourism. These LiDAR data consisted of original data and ground data of the ground surface. Since it was detected that the ground data did not represent detailed topography, the topographic analysis was conducted using the original data. First, the original text data were converted to a las file, using R software version 4.0.1 (R Core Team, 2021), and only the ground surface was extracted from the point cloud data using the lidR package.

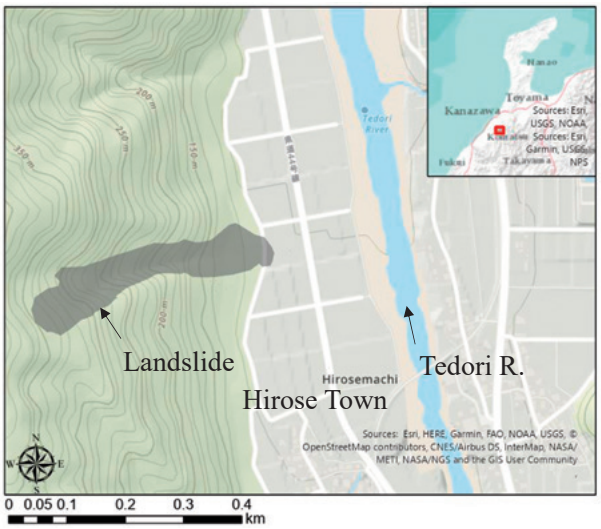

Figure 1: Location of Hirose Landslide (cited from ArcGIS online topographical map)

Figure 2: Panoramic view of the collapsed area taken from helicopter

Then, this point cloud data was used to create a 0.5m mesh DTM data and saved as a GeoTIFF file using the raster package function. Second, a detailed 1-meter contour topographic map of the post-collapse topography was utilized (provided by the Ishikawa Prefecture Forest Management Division, Ishikawa Prefecture, Japan), to create a 0.5-meter DEM file using ArcGISPro 2.8 and saved as a GeoTIFF file. These two GeoTIFF files were used to estimate the amount of topographic change, the amount of sediment produced, and deposited using the raster calculation tool and the CutFill tool in ArcGISPro 2.8.

The original data and the ground surface data were further used to estimate the number of trees that were grown in the collapsed area before the landslide. The CHM tool in the lidr package was used to differentiate the canopy data from the original data and the ground surface data, by determining the vertices to obtain the height of each single tree as point data. Further clipping with the polygon of the collapsed area, the number of trees that had been buried and deposited by the landslide were estimated.

Additionally, a drone (Mavic2 Zoom) captured imageries were used to measure the post-collapse microtopography and size (height) of driftwood. For capturing pictures, the collapsed area was divided into three sections. The shooting range and altitude were set using the GroundStationPro application, and the automatic shooting mode of drone was activated. Drone photography was conducted in June 2021, one month after the landslide. The photos taken were processed to create orthophotos, DTMs, and DSMs in the laboratory using ESRI's Drone2Map for further assessment.

In order to understand the sediment runoff prevention function of trees lost during the collapse, the Critical Turning Moment (Y) is calculated using the average height and DBH of the estimated lost tree. The 'Y' depends directly upon the size of the DBH. This 'Y' was assessed for each lost cedar tree by using an equation prepared for cedar trees by Shimada and Nonoda (2017) as below.

$Y = 19.84X \ldots\ldots\ldots\ldots\ldots\ldots\ldots\ldots$ equation (1)

Where, Y is the Critical turning moment (kNm)

and $X = H \times DBH^2$

Here, H = Tree Height, and $DBH = 0.3914 \times H^{1.407}$

DBH = Daimeter at Breast Height (cm)

However, since the LiDAR data was collected in 2006, there is a time lag of 15 years from 2021, the date of the landslide event. Therefore, we estimated the height of Cedar trees after 15 years by referring to the height growth curve of Cedar trees by Kotani and Sengi (2006) and DBH is calculated further to obtain the critical turning moment in 2021.

2) Field survey

Field surveys were conducted in May, June, and August 2021. A 10 x 10-meter quadrat was set up in the planted Cedar Forest growing in the vicinity of the site, and the DBH, height, and understory herbs of the trees within the quadrat were measured. Next, topographic measurements were taken in the collapsed area, and the size of driftwood was measured using a measuring staff. Soil samples were collected at the source head of the collapsed site.

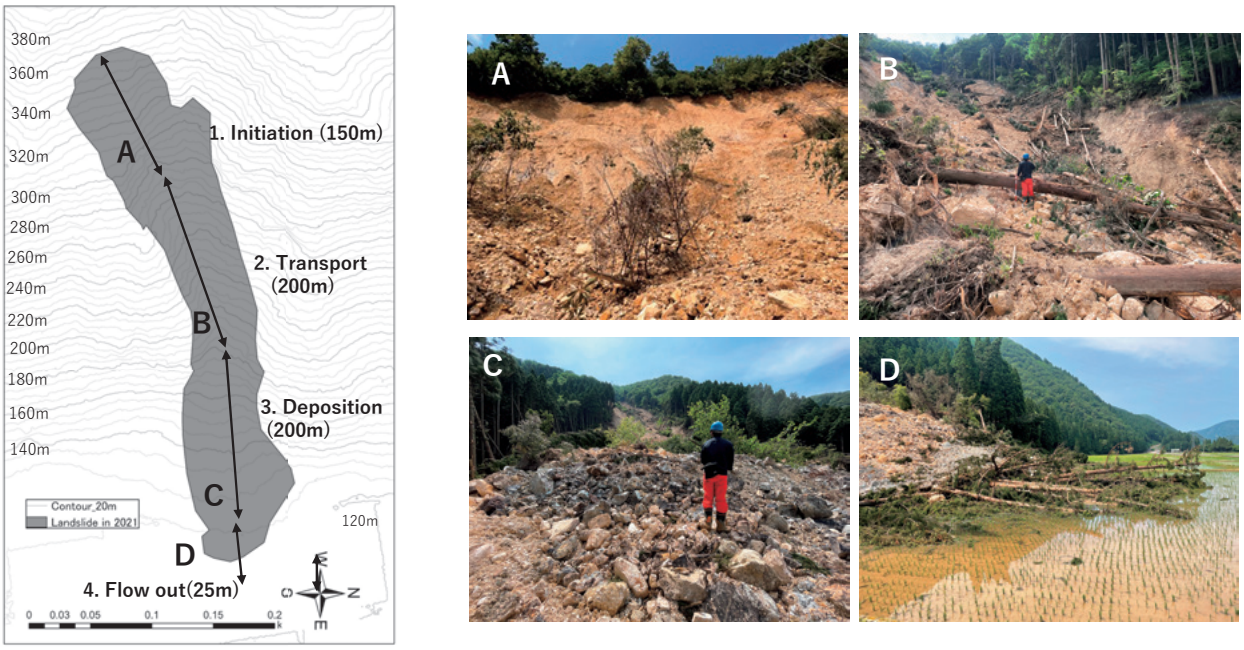

Figure 3: Landslide morphology and its classification: landslide topography with contours (20m) and sediment run-off distance (left); A) debris production (Initiation); B) middle section with toppled trees and driftwood (Transport); C) depositional area with debris (Deposition); D) toe of landslide near paddy fields (Flow out)

For understanding the local resident's perception of the situation before and after the landslide, nearly half of the households (n=16 samples, out of 34 households) were interviewed. We collected their views by asking a few questions such as a) if there were any unusual events or signs noticed along the slope prior to the collapse; b) how much rainfall occurred in that period; c) is this landslide resulted from the activation of older collapse? and d) when was the Cedar plantation conducted? One of the residents, who were working in the agricultural field directly below the collapsed site on the day of the landslide incident, shared noteworthy experiences regarding the Hirose Landslide event.

3) Laboratory analysis of soil sample to estimate sediment mobility index

For the clay layer contained in the collapsed sediment, the clay sample was taken back to the laboratory, 10 mL of 0.5 mol/L magnesium chloride solution was added to approximately 0.5 g of the clay sample, stirred well, and allowed to stand overnight (Mg saturation treatment). After stagnating, the magnesium chloride solution was removed by centrifugation (2,000 g, 15 min). Then, 10 mL of ultrapure water was added, stirred well, and centrifuged (2,000 g, 15 min) to remove the supernatant solution. This washing operation with ultrapure water was performed twice to remove excess magnesium that was not adsorbed on the clay sample. The same washing operation was then performed twice with ethanol to replace the solvent from water with ethanol. The Mg-type clay sample (solvent: ethanol) was prepared by the above operations. To this, 1 mL of ethanol was added, and the clay sample in suspension was applied to a preparate and dried at room temperature. Ethylene glycol was applied to this preparate and the dried sample (EG-treated), a sample heated at 300° C for 1 hour using a muffle furnace (heat-treated), and an untreated sample (Mg-saturated) were prepared for X-ray diffraction (XRD). The XRD system used was a Rigaku MiniFlex with a copper tube sphere. The measurement conditions were as follows: tube voltage 30 kV, tube current 15 mA, measurement range 5 to 30°, step width 0.1°. The lattice spacing (nm) was calculated from the obtained diffraction angle (2θ) and X-ray wavelength (λ = 0.15418 nm) using the Bragg formula.

The saturated water content ratio and liquid limit of the collapsed clay were measured, and the approximate mobility index, which was proposed by Ellen et al. (1987) as an index of the mobility of collapsed clay, was calculated. The approximate mobility index is expressed as the ratio of the saturated water content ratio to the liquid limit

(Yamashita et al., 1992).

3. Results

(1) General characteristics of collapse

Figure 3 shows a plain view of the collapse that occurred in the Hirose area and the situation in each section from debris production (initiation) area to the toe (flow out) area (3A, B, C, D). The total length of the landslide terrain reached 575 m. The initiation area was 78 m wide and 150 m long between 280 and 360 m above sea level, with a collapse area of 1.1 ha. The length of the exposed bedrock is about 40m, and the slope is steep with an angle of over 40°. The base of the slope was flat and mortar-shaped, and medium-sized hardwood trees with roots had slid down and accumulated in the center forming a board-like shape (40 m wide and 60 m long) (Figure 3, A).

The lower part of the valley is a steep slope where collapsed sediments move (Transport zone), with an elevation of 180 to 280 m, a width of 50 m, a length of 200 m, and a slope of 35 to 40°. The central part of the valley was cut off like a slough, and highly viscous mud mixed with spring water and clay was flowing down. At the base of the valley, more than a dozen large-diameter Cedar trees (root diameter of 50 cm or more), which had fallen secondarily after the mudslide, were observed (Figure 3B).

In the deposition area, huge gravels reaching 50 cm~2 m in diameter were deposited on an alluvial cone which lies at 120-180 m above sea level. The deposition area was 70 m wide, 200 m long, and with a slope of about 15°. The deposits had a lobed topography and were layered downstream (Figure 3, Photo C). Its terminus bordered a planted Cedar Forest, which was dammed up to a height of 5 m as the mudslide drifted the Cedar Forest at the terminus. Along its edge, many driftwoods were continuously deposited in overlapping rows for a length of 200 meters.

There was a farm road as a seprating boundary between the rice field and the forested area. The debris flow completely covered the road, forming a small hill-like terrain and deposit the debris. The debris flow of landslide overhung the paddy field side about 25 m from the end of the road. A few Ceder trees that had been toppled down and reached almost to the road with debris flow.

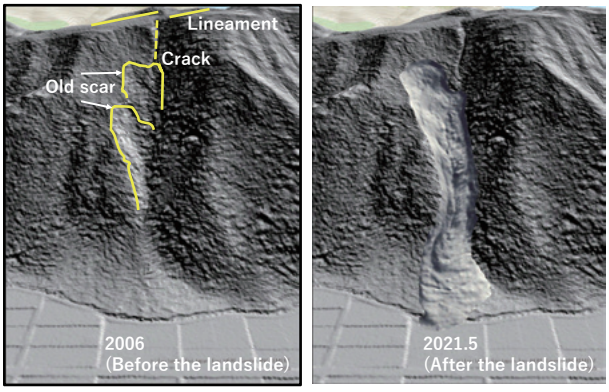

Figure 4: Comparison of geomorphological change before and after the landslide by LiDAR analysis

(2) Terrain analysis using LiDAR data

LiDAR data, taken in 2006, before the collapse were analyzed to reconstruct the pre-collapse topography. Figure 4 shows the shaded relief map created from the topographic survey before 2006 on the left and after 2021 the collapse on the right. The slope around the head scarp where the collapse occurred had a concave catchment topography with steep slope before the collapse. In this zero-order valley, two previously collapsed slope were identified in the middle to upper part of present landslide slope. The first one developed at an elevation of 300 m on the right side of the slope and was 150 m long and 50 m wide. The second is a 50m wide and 100m long collapse zone at an elevation of 340m above the slope.

A clear alluvial cone with a radius of 110 m and an angle of 105° was formed at the bottom of the slope, and its end overhung the alluvial surface (terrace). The debris flow spread and deposited (Flow out zone) from the center of the cone, which was 150 m long and at a narrow angle of 45°.

(3) Topographic change and sediment budget

Figure 5 (left) shows a plan view of the difference in elevation before and after the collapse, and the right shows the topographic changes before and after the collapse in the production (initiation) area (Line A), downstream sliding (transport) area (Line B), and deposition area (Line C). In the initiation area, the maximum elevation was depleted by 22 m, and the average elevation was reduced by about 15 m, indicating that arc-shaped slides occurred in the entire area. In the downstream area, the V-shaped valley topography was buried and flattened by about 6m. In the landslide flanks, the slopes were depleted by

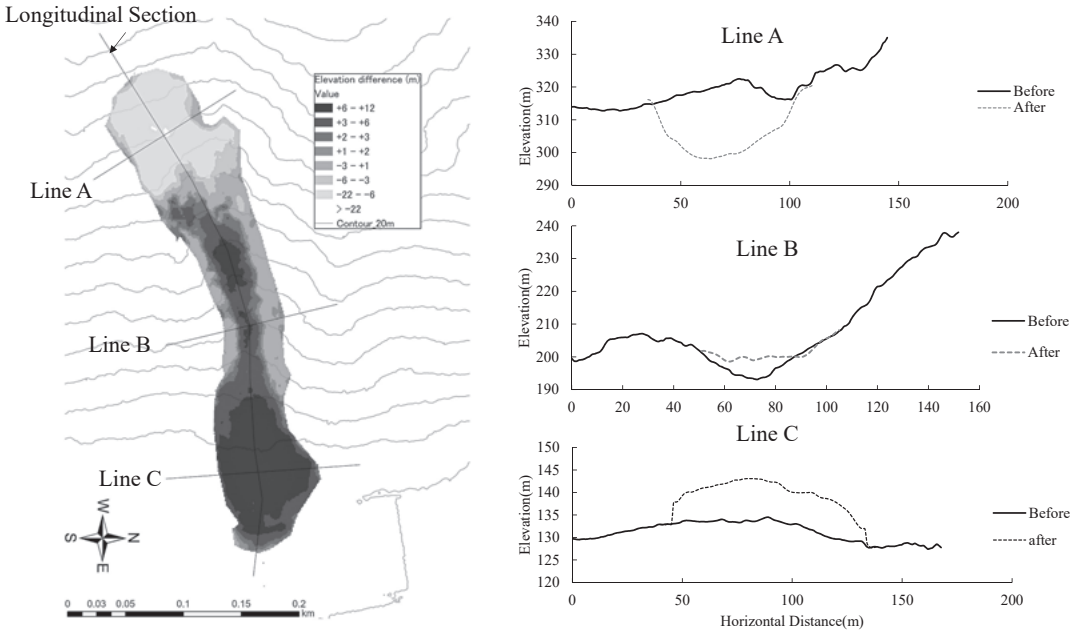

Figure 5: Topographic surface changes before and after collapse in three sections: Initiation section-Line A, Transport section-Line B, and deposition area-Line C

about 1 m. In the depositional area, the collapsed soil was deposited in a convex shape with a thickness of about 8 m over an area of about 80 $m^{2.}$

The changes in the longitudinal topography before and after the collapse are shown in Figure 6. The slope before the collapse at an elevation of 300~350m is considered to be an old landslide block, and a concave break point can be recognized. In the present case, the upper slope above the transition line collapsed with a 15m-deep arc-shaped slip surface. In the downstream area from 160m to 300m elevations, sediments cover the slope, and as shown in Figure 5, Line B, the V-shaped valley floor is filled with sediments. Below the elevation of 160 m, the area is a depositional area, and the mudslide that flowed downstream overshooted the end of the alluvial cone and advanced further to the rice paddy field, and stopped. The volume of sediment produced by the landslide in the initiation area was 86,000 m^3, while 22,000 m^3 was deposited in the transport area, 3000 m^3 was scoured from the valley walls in the transport area, and 63,000 m^3 was deposited in the deposition area. Out of the 89,000 cubic meters of sediment produced, 85,000 cubic meters were transported as debris and 4,000 cubic meters were discharged from the watershed with flowing water.

(4) Driftwood distribution and forest sediment runoff control function

Figure 7 shows the number of trees and their height distribution in the collapse area estimated based on the distribution of Cedar plantation forest shoot tips

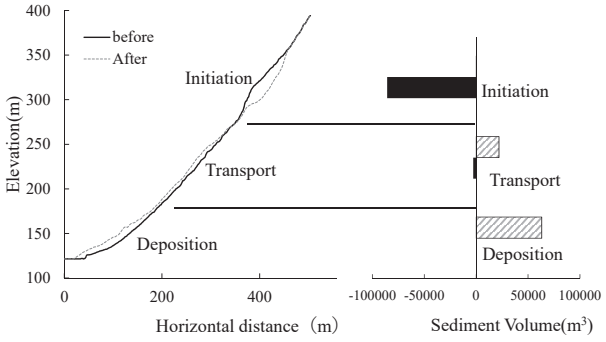

Figure 6: Longitudinal profile change and sediment production

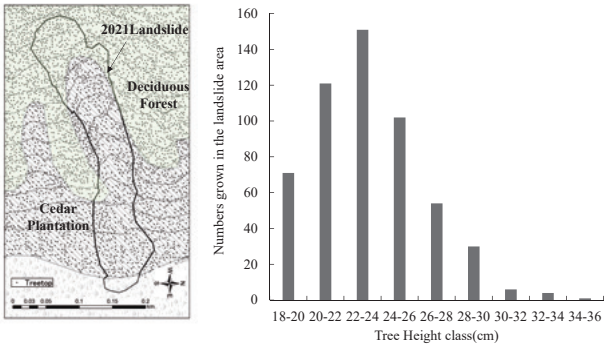

Figure 7: Tree height frequency distribution of planted Cedar Forest before the landslide

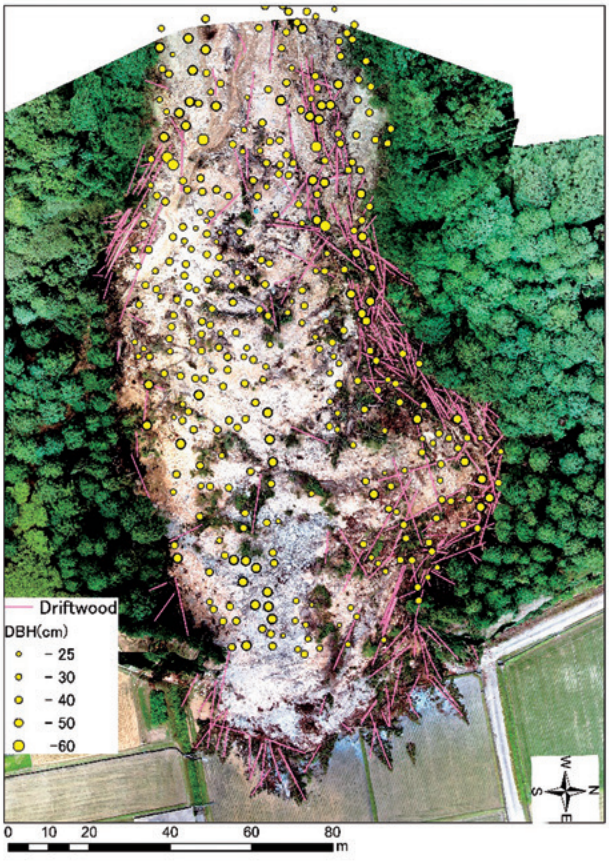

Figure 8: Landslide photo showing driftwood and Cedar trees. Yellow circles indicate the combined location and DBH (cm) of Cedar trees that were destroyed by landslide

before the collapse. Most of the upper slope was covered with secondary broadleaf forest. However, most of the middle-downstream and sedimentation areas were covered with Cedar Forest, with average height of 22-24 m, and a few exceeding 30 m. The number of trees and their height frequency distribution are shown in Figure 7. The DBH for all the 540 Cedar trees was estimated and the critical turning moment was calculated. The critical turning moment calculated by equation (1) is 59.3 kNm per tree and overall is 32067 kNm. When this value was recalculated based on the estimated tree height in 2021, 15 years later, it was found that the total turning resistance was 73069 kNm, almost double to the turning resistance of 2006.

Figure 8 shows an orthorectified aerial photograph taken by a Drone over the deposition area. The Cedar Forest in the collapse area has been severely destroyed by the mudslide, and driftwood has accumulated as if swept up around the mudslide. The circles in the Figure 8 indicate the location and size of Cedar trees

Figure 9: Sediment accumulation by "retention-dam" like structure of driftwood observed in the sedimentation area

that were distributed before the collapse. The main source of the driftwood accumulated on the left bank is the Cedar Forest that was distributed along the flow path (initiation, transport, and deposit). The central part of the landslide area was sparsely forested but occupied with large-diameter sized Cedar trees. These trees were buried by the debris flow, and their tips were slightly exposed on the ground surface. Their arrangement was consistent with the sedimentary structure of the debris flow, and they were distributed in an arc along the lobe-shaped topography (Figure 8). The number of Cedar trees that existed in the initiation, transport, and the deposit area was determined to be 540, out of which 230 trees were deposited as driftwood on the ground surface. The remaining, 310 trees, are estimated to be buried in the debris flow material and not visible.

Figure 9 shows the accumulation of driftwood at the end of the left bank. The roots of these driftwood has diameter of 84 cm on maximum and 46 cm on average, forming a retention dam-like structure up to 8 m high and storing a large amount of sediment behind it.

(5) Rainfall and interviews with local residents

Figure 10 shows the daily and hourly maximum rainfall before and after the collapse. On May 20, 2021, when the landslide occurred, the rainfall was 11.5 mm and the maximum hourly rainfall was only 3 mm. Prior to this, there was rather heavy rainfall on May 17, with a daily rainfall of 105 mm and an hourly rainfall of 11.5 mm at 8:00 a.m. From then until May 20, there was only a little amount of

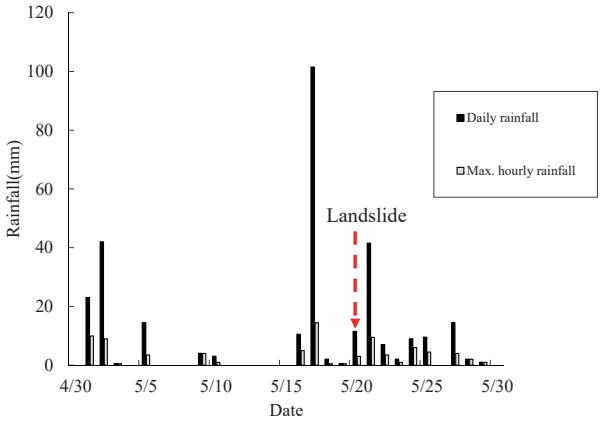

Figure 10: Daily and hourly maximum rainfall before and after the landslide (May 2021). Source: Japan Meteorological Agency (2021)

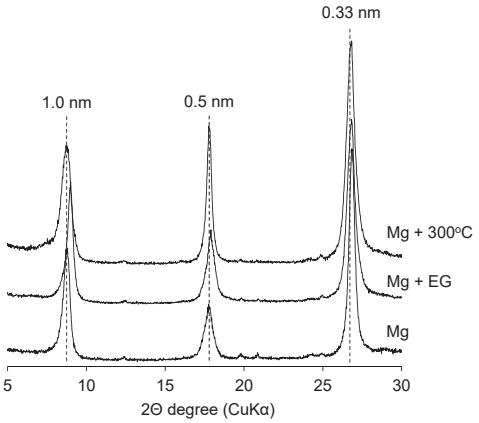

Figure 11: Results of clay mineral analysis of sampled soil

rainfall with a maximum daily rainfall of 10 mm. However, in early May, there was rainfall of 15-42 mm per day.

Interviews (random interaction) were conducted with the Hirose town residents regarding the occurrence of the landslide. Most of the interviewees recalled that no previous movement or cracks were noticed in the hillslope, however, they highlighted that there was intense rainfall in the area 3 days before the event. Some interviewees mentioned that the area was a bare landscape with fewer trees in the past and the plantation of Cedar trees was implemented by local government authorities.

In particular, the local farmers (About 50 years old) shared his experience:

"I was working on my agricultural farm in the same area just one day before (May 19), but there was nothing unusual (not even a sound). However, a few days before (May 17), we experienced heavy rainfall and trees were swaying along the head region of the landslide. On that day (May 20), I was wearing a raincoat and working around my house as there were occasional light showers occurring since morning. Just before the landslide (May 20, 2:30 pm), there was strange rumbling and crackling sound (like a loud explosion) was heard. Immediately, the collapse occurred and a huge earth mass with rocks and sediment was knocking down the Cedar trees and flowing downwards. That event lasted within 15-20 seconds and within a short time, the dusty smoke covered this area. I also felt the smell of soil and broken wood. Then after some time, another small failure occurred with lesser sediment originating at the head section of the landslide."

The information about the reoccurrence of two separate collapses was triangulated with several other residents during the interview. It seems that a deep collapse occurred first and then some unstable slopes fall near the head region of the landslide.

According to a male (80 years) respondent: "This Hirose hill slope area was once denuded and in the late 1950s and 1960s Cedar trees were planted by the government authorities together with local communities. He mentioned that the forest area had been used to harvest timber and fuelwood in the early 1950s and already collapsed twice before the Cedar trees plantation campaign was organized."

(6) Mineral composition and physical properties of clays in collapsed sediments

Figure 11 shows the XRD patterns of the clay samples; the lattice plane spacing calculated from the peak positions of the XRD patterns of the Mg-saturated samples were 1.0 nm, 0.5 nm, and 0.33 nm, consistent with those of illite. Furthermore, the peak at 1.0 nm, corresponding to the 001 plane of clay minerals, did not change with EG or heat treatments, which is also consistent with the characteristics of illite (Shiramizu, 2010). In addition, for hydrohaloysite, which, like illite, has a peak near 1.0 nm, (1) the peak shifts from 1.0 nm to 0.7 nm due to dehydration associated with heat treatment, and (2) the peak shifts from 1.0 nm to 1.1 nm due to expansion of the interlayer by EG treatment (Joussein et al., 2005). In summary, the mineral species is very likely illite, since the XRD pattern of this sample is consistent with that of illite, and the above peak shift was not confirmed for the 1.0 nm peak.

The results of the liquid limit test are shown in

Table 1. Since the liquid limit is defined as the water content ratio at 25 fall times, an approximate curve of fall times and water content ratio was developed from this table to estimate the liquid limit. The physical properties of the collapsed clay are shown in Table 2. The liquid limit was 45% and the saturated water content ratio was 65%. From the liquid limit and saturated water content ratio, the fluidization index was calculated to be 1.4, which clearly exceeds 1. Therefore, the clay was determined to have an easily fluidizable property.

Table 1: Result of liquid limit test

Number of fall	42	30	22	13
Water content (%)	39.6	43.1	46.3	47.7

Table 2: Physical property of collapsed clay

liquid limit (%)	saturated water content	fluidization index
45	65	1.4

4. Discussion

(1) Mechanism of deep-seated landslide

The deep landslide that occurred near Hirose town reached a slope failure depth of 22 m, with a total collapse area of 1.1 ha, and produced sediment volume of 86,000 m^3 from the main collapsed zone. According to Hatanji (2003), deep-seated collapses that occurred between the 1960s and 1990s varied in size from 4 to 3.7 million m^3, and the maximum depth of collapse was reported to be 17 to 100 meters. In this case, the Hirose landslide is classified as one of the relatively smallest deep-seated collapses in this region. In the Tedori River basin, a landslide-occurred in 2015 during the snowmelt season in Sennin-dani upstream of the Ozoe River, and the volume of soil was reported to be 1.3 million m^3 and the maximum depth of collapse was 45 m (Yanai, 2017). Also, in the upper reaches of the Ushikubu River in the Tedori River basin, the Betto giant Collapse (1.64 million m^3 of collapsed soil) occurred in 1934 (Wang and Sassa, 2007). Hirose landslide was small in comparison to those events, however, it occurred in the lower reaches of the river near a human settlement with cultivated lands, the extent of its impact was large.

The source of the collapse was a steep slope in the upper 280-360 m elevation range, and LiDAR data taken prior to the collapse showed evidence of a sliding bedrock. Interviews with nearby residents also revealed that sediment was released from the slope previously once in the 1950s. Therefore, the present collapse is predicted to be the collapse of an unstable weathered layer on the slope. According to Daimaru et al. (2013), deep-seated collapses in the middle basin of the Oigawa River are followed by a preceding collapse on both slopes, and they report that there are two types of collapses: a type in which a small-scale preceding collapse occurs at the foot of the slope that begins to expand before the collapse occurs (extrusion type) and a type in which the collapse area expands rapidly toward the upper side of the slope of the preceding collapse (expansion type). Thus, the tendency for large-scale collapses to occur after a preceding event is evident.

Linear depressions (depressions roughly parallel to a mountain ridge) are explained as point where deep failures occur (Chigira, 2015). These depressions may form almost symmetrically on both sides of a mountain ridge, or they may develop on one side of a mountain ridge, or, although sometimes rare but they may form singly on a mountain ridge. Jitousono (2005) and the Volcanic and Debris Flow Team (2008) also noted that lineaments and linear depressions are key to predicting the location of a collapse. In the study area, the upper part of the landslide had a gentle slope on a ridge, and linear lineaments and depressions had developed between the ridge and the slope. The ridge-top slope had a clear crack extending from the ridge to the slope, suggesting that a subsurface fault had formed and destabilized the area.

Jitousono (2005) and Jotousono et al. (2006) pointed out that if the lineament is a fault, it is likely to be fractured in deep Sub-surface, and there may be a thick layer of weathering. Takeshita and Shimizu (1997) also pointed out the need for deep stratification of the mountain body and the existence of brittle basement rock. Rainfall takes time to pass through such thick weathered layers, and there is often a delay between the peak of rainfall and the onset of collapse (Onda et. al., 1999, Hattanji, 2003). The delay usually ranges from 20 to 150 hours, but in the case of the Hirose landslide, it took a relatively long time, 78 hours after the peak rainfall. This is thought to be caused by the time required for the groundwater table to rise due to passage through a very thick weathered layer as shown in Figure 3-A.

Analysis of clay minerals exposed on the collapse surface revealed that illite was the predominant mineral. According to Maeda et al. (2011), geological characteristics of hydrothermal alteration zone landslides occur mostly in the potash feldspar and illite zones. The Kawai Mine, where the ceramic stone used to make Kutani ware is sand bedded, is located 1 km southwest of the Hirose Landslide area, and the surrounding andesite and rhyolite are widely altered. Since the liquid limit of this clay layer is smaller than the saturated water content (i.e., the fluidization index exceeds 1), it is expected to become liquid and easily fluidized as this clay layer approaches its saturated water content due to rising groundwater. It is highly likely that the clay layer that underwent this alteration was used as a slip surface and that a deep collapse occurred. Under these geological conditions, in this area where there are many lineaments and faults, it is possible that similar deep failures may occur in the future.

(2) Quantifying the effectiveness of Cedar trees for debris flow control

Several recent large-scale landslides have been reported in which mudslides have uprooted large amounts of driftwood, which often indicated good information about discharged sediment. For example, according to Todo et al. (2015), in the 2009 landslide in northern Harima and southern Tajima, Hyogo Prefecture, when the fluid, which was a combination of driftwood and sediment, passed through a comb or grid slit, a “sieving function” has activated, allowing water to pass through the slit, while driftwood and sediment were separated and deposited on the upside of the slit. This function reduced the destructive energy of the flow, and the debris-flow reduction function was reported.

Nonoyama et al. (2020) reported that mudslides generated by torrential rains that hit Hiroshima Prefecture in 2018 were deterred by the formation of lobes (tongue-shaped sedimentary landforms) due to collisions with standing trees. Even in small tree forests at the foot of mountains functioned to reduce subsequent sediment flow and diverted towards the flat surface. Hirose landslide investigation assured that Cedar trees on the slope deterred sediment from flowing down as fallen trees intercepted the mudslide by storing sediment and eventually staying there as driftwood.

In the case of Hirose landslide, the sediment produced by the deep failure flowed down the steep slope and diffused into the alluvial cone, pushing down a well-established Cedar Forest (average diameter at breast height 48 cm, height 28 m) that was growing along the slope, and it is assumed that the flow energy was mostly reduced during this process. The traces of this can be inferred from the fact that the Cedar trees that were distributed there were deeply buried as shown in Figure 8, and their treetop ends are aligned along the top of the debris flow lobe. The amount of energy required to pull down a tree is highly correlated with its DBH (Fukami et al., 2011; Shimada and Nonoda, 2017), and a tree having a DBH of 40cm, requires approximately 80 kNm of energy to be pulled down. Therefore, we estimated the DBH from the height of 540 Cedar trees which were destroyed during collapse. By applying Shimada-Nonada formula, the strength of total lost Cedar trees was calculated. The calculated strength is approximately 73069 kNm, which has resisted the debris flow to spread down to the agricultural field in the alluvial fan. The moment of resistance to pulling down a standing tree is negatively correlated with tree density (Fukami et al., 2011), and increases exponentially with breast height diameter, meaning that it is important for disaster prevention that small diameter trees should be appropriately thinned out to create forests of large diameter trees.

On the other hand, another important disaster mitigation function observed this time was that the standing trees captured the driftwood that flowed down like vertical piles and accumulated to serve as a retention-dam-like structure, storing a large amount of collapsed sediment behind them. The width of the dam reached 120 m on the left bank, and its height was up to 8 m. Driftwood spilled by mudslides is a nuisance in terms of disaster prevention, as it can get caught on bridge piers, blocking the flow of the river and causing flooding (Mizuhara, 2016). However, during the 2018 mudslide disaster in Hiroshima Prefecture, it was reported that sediment was deposited up to 1~3 m thick by driftwood dams (Nonoyama et al., 2020), which is much smaller than the Hirose Landslide. The major difference from the Hiroshima Prefecture case is that the Cedar plantation in the Hirose area had large-diameter trees (approximately 48 cm), which were able to withstand

and maintain the soil pressure behind them. In the case of the debris flow in Hiroshima, a large amount of water from torrential rains and large rocks containing large debris flowed over a long distance, whereas in the Hirose Landslide, the amount of water was less, and the distance traveled by the rocks was shorter, so the large-diameter Cedar trees probably functioned effectively as a deterrent to debris flow.

It has been experimentally confirmed that in a mountain stream, driftwood included in a mudslide gets trapped when it passes through a section with standing stems, which supports the subsequent trapping of sediment and driftwood one after another, forming a channel blockage and causing the stream to divert in a short time (Hasegawa et al. 2016). Sediment stored by driftwood-dam is often considered to amplify disasters, but in open landscapes, it should be considered to examplify its contribution to disaster mitigation. As previous disasters have already demonstrated that there are no such engineering techniques that are completely safe and disaster-proof (Kato and Huang, 2021). Also considering the low cost and multifaceted benefits, one of the best ways to reduce landslide risk is to create a forest ecosystem by planting trees along slopes prone to collapse. This can be a sustainable and cost-effective ecosystem-based solution to reduce the risk of landslide disasters in similar geological settings (Moos et al., 2018).

At the same time, from the perspective of disaster mitigation, it is also important to grow forests in areas such as alluvial cones, which were formed by past collapses and are likely to experience landslide in the future. It is therefore recommended to document and quantify the role of forest-based techniques to mitigate the risks of landslides in order to assess their suitability for specific locations and to ensure that they are implemented correctly.

Acknowledgement

The Ishikawa Agriculture and Forestry Office, Forestry Division, and the Forest Management Section of the Ishikawa Prefecture Agriculture, Forestry, and Fisheries Department provided survey data on the collapsed area. In addition, residents of Hirose-town, Hakusan City, provided much cooperation during interviews about the landslide status. In addition, graduate students and students from the Laboratory of Watershed Environmental Studies in the Department of Environmental Science assisted with field surveys and soil sample preparation. We would like to express our deepest gratitude to all of them.

References

Asada, H, Minagawa, T, Koyama, A and Ichiyanagi, H. 2020. Analysis of Factors Contributing to Surface Failure on Slopes Caused by the July 2017 Torrential Rainfall in Northern Kyushu, Japan. Applied Ecological Engineering. 23. 185-196.

Chigira, M. 2015. Prediction of deep collapse locations and future research development. Applied Geology. 56. 200-209.

Daimaru, H, Kurokawa, U, Murakami, W and Matsuura, J. 2013. Geomorphological characteristics of deep-fall occurrence slopes in the Sento area based on multi-temporal geographic information. Journal of the Landslide Engineering Society of Japan. 50. 24-33.

Ellen, S, D and Fleming, R, W. 1987. Mobilization of debris flows from soil slips, San Fransisco Bay region, California, Geological Society of America Reviews in Engineering Geology. 7. 31-40.

Fukami, Y, Kitahara, Y, Ono, H, Toudou, C and Yamase, K. 2011. Stand Pull-down Test under Different Conditions of Soil Moisture. Journal of Forest Science Society of Japan. 93. 8-13.

Hasegawa, Y, Satomi, Y and Mizuyama, T. 2016. Experiments on the Formation and Failure of a River Channel Blockage by a Mudflow Containing Driftwood. Journal of Erosion Control Society of Japan. 69. 19-23.

Hatanji, T. 2003. Characteristics of rainfall-induced deep failures, Journal of Erosion Control Society of Japan. 55 (6). 74-77.

Ishikawa Prefecture. 1987.Fundamental Land Classification Survey, Tsurugi.

Jitousono, T. 2005. Deep Failure. Journal of Erosion Control Society of Japan. 58. 60-66.

Jitousono, T, Shimokawa, E and Teramoto Y. 2006. Proposal of a Prediction Method for Deep Failure Sites. Journal of Erosion Control Society of Japan. 59. 5-12.

Joussein, E, Petit, S, Churchman, J, Theng, B, Righi, D and Delvaux, B. 2005. Halloysite clay minerals-a review. Clay minerals. Clay minerals. 40. 383-426.

Kaibori, M, Hasegawa, Y, Yamashita, Y, Sakita, H, Nakai, S, Kuwata, S, Hiramatsu, S, Jitousono T, Irasawa, M, Shimizu, S, Imaizumi, F, Nakatani, K, Kashiwabara, Y, Kato, N, Torita, E, Hirakawa, Y, Yoshinaga, S, Tanaka, K and Hayashi, S. 2018. Landslide Disasters in Hiroshima Prefecture Caused by Heavy Rainfall in July, 2008.

Journal of Erosion Control Society of Japan. 71. 49-60.
Japan Meteorological Agency. Ishikawa Prefecture Hakusan River Area Meteorological Data (viewed August 20, 2021) (https://www.data.jma.go.jp/obd/stats/etrn/index.php?prec_no=56&block_no=0973&year=2021&month=05&day=20&view=g_pre).
Joussein, E, Petit, S, Churchman, J, Theng, B, Righi, D and Delvaux, B. 2005. Halloysite clay minerals — a review. Clay minerals. 40. 383-426.
Kato, S and Huang, W. 2021. Land use management recommendations for reducing the risk of downstream flooding based on a land use change analysis and the concept of ecosystem-based disaster risk reduction. Journal of Environmental Management. 287. 112341.
Kitahara, Y. 2010. Collapse prevention function of forest root systems. Water Science. 53. 11-37.
Kotani, J and Sengi, Y. 2006. Estimation of site index and stem quality in old Cryptomeria japonica plantations by factors of site environment. Ishikawa Prefectural Forest Experiment Report. 38. 16-20.
Maeda, H, Natani, H, Uematsu, S and Kono, K. 2011. Geological characteristics of hydrothermal alteration zone landslides: Example of Ikutawara-minami landslide area, Hokkaido. Journal of the Landslide Engineering Society of Japan. 48. 139-146.
Matsumura, K, Fujita, S, Yamada, T, Gonda, Y, Numamoto, S, Tutsumi, D, Nakatani, K, Imaizumi, F, Shimada, T, Kaibori, M, Suzuki, K, Tokunaga, H, Kashiwabara, Y, Nagano, E, Yokoyama, O, Suzuki, T, Takezawa, N, Ohno, R, Nagayama, T, Ikejima, T, Tsuchiya, S. 2012. Landslides in the Kii Peninsula caused by Typhoon No.12 in September 2011. Journal of Erosion Control Society of Japan. 64. 43-53.
Mizuhara, K. 2016. A Study on Disasters Caused by Driftwood Associated with Mudslides and Measures to Prevent and Mitigate Them. Water Science 60. 1-46.
Mizuyama, T, Kurihara, J and Suzuki, H. 1990. Impact energy absorption effect of standing trees. Journal of Erosion Control Society of Japan. 42(6). 24-28.
Moos, C, Bebi, P, Schwarz, Stoffel, M, Sudmeier-Rieux, K and Dorren, L. 2018. Ecosystem-based disaster risk reduction in mountains. Earth-Science Reviews.177. 497–513.
Nonoyama, K, Ikeyama, T and Yamane, M. 2020. Effects of forests on sediment discharge reduction in mudslides caused by the July 2008 heavy rain disaster in Hiroshima Prefecture, Japan. Water Science. 64. 21-42.
Onda, Y, Komatsu, Y, Tsujimura, M and Fujiwara, J. 1999. Prediction of the time of collapse occurrence from the difference of delay time of rainfall-runoff peak. Journal of Erosion Control Society of Japan. 51. 48-52.
R core team. 2021. R: A language and environment for statistical computing. R Foundation for Statistical Computing, Vienna, Austria. https://www.R-project.org/.
Shimada, H and Nonoda, T. 2017. Pull-down resistance of cedar and cypress stands in the central region of Mie Prefecture. Journal of the Japanese Society of Arboricultural Engineering. 43(1). 138-143.
Shiramizu, H. 2010. Clay Mineralogy - Basics of Clay Science. Asakura Shoten.
Takeshita, K and Shimizu, A. 1997. Deep Failure of the Left Bank of the Aburatani River, Sakamoto Village, Kumamoto Prefecture, Japan (Preliminary Report). Journal of Erosion Control Society of Japan. 50. 77-80.
Todo, C, Yamase, K, Tanigawa,H, Ohashi, M, Ikeno, H, Dan'ura,M and Hirano, Y. 2015. Special Issue on "Disaster Prevention Revegetation and Landslide Disaster "Effect of Thinning on Maximum Pull-down Resistance Moment of Japanese Cedar. Journal of the Japanese Society for Afforestation Engineering. 41. 308-314.
Volcanic and Debris Flow Team, Sediment Management Research Group, Public Works Research Institute. 2008. Manual for Identifying Streams at Risk of Deep Failure (Draft). Public Works Research Institute data.4115.
Wang, F, and Sassa, K. 2007. Initiation and Traveling Mechanisms of the May 2004 Landslide—Debris Flow at Bettou-Dani of the Jinnosuke-Dani Landslide, Haku-San Mountain, Japan. Soils and Foundations, 47(1), 141–152.
Yamashita, Y, Ishikawa, Y and Kusano, S. 1992. Soil properties of collapsed areas at the source of debris flow, Japan. Journal of the Japanese Society of Arboricultural Engineering. 44 (5). 19-25.
Yanai, S and Igarashi, Y. 1990. History of the Slope Failure and Paleoenvironment on the Marine Terrace of Hidaka District, Central Hokkaido. The Quaternarily Research. 29. 319–336.
Yanai, S. 2017. Landslide and turbid water in the headwaters area of Mt. Hakusan in May 2015. Water Science 61. 75–91.

深層崩壊の特徴とスギ林の土砂流出防止機能

石川県白山市広瀬町に発生した地すべりの事例

Prakash S. Thapa（石川県立大学 大学院自然共生科学専攻）
半澤風人（ドーコン，石川県立大学 環境科学科 2021年卒業）
勝見尚也（石川県立大学 生物資源環境学部 環境科学科）
百瀬年彦（石川県立大学 生物資源環境学部 環境科学科）
柳井清治（石川県立大学 名誉教授）

要　旨

2021年5月石川県白山市広瀬町で大規模な深層崩壊が発生した。そこでLiDARデータ，現地測量データおよびドローンを用い，深層崩壊の実態を解析した。その結果，崩壊源の深さは約22m，崩壊面積は約11,000m^2，生産土砂量は約86,000m^{3}であった。崩壊斜面周辺には線状凹地とリニアメントが発達しており，地下水位が上昇するのに時間を要したため，先行降雨から78時間後に崩壊が発生したと考えられた。崩壊土砂は流下する過程で土石流となり斜面上のスギ林を破壊しながら約475m流下した後，沖積錐上に拡散堆積した。土石流の末端では流木が約8mの厚さでダムアップし，背後に多量の土砂を貯留して停止していた。土石流の流出が抑制された要因として，スギ人工林の引き倒し抵抗モーメントによる減勢と流木ダムによる貯留効果が考えられた。

キーワード：深層崩壊，スギ人工林，流木ダム，土砂流出防止機能，LiDAR